[CANCER RESEARCH 63, 4450–4459, August 1, 2003]

The Biological and Biochemical Effects of CP-654577, a Selective erbB2 Kinase Inhibitor, on Human Breast Cancer Cells

E. Gabriella Barbacci, Leslie R. Pustilnik, Ann Marie K. Rossi, Erling Emerson, Penny E. Miller, Brian P. Boscoe, Eric D. Cox, Kenneth K. Iwata, Jitesh P. Jani, Kathleen Provoncha, John C. Kath, Zhengyu Liu, and James D. Moyer[1]

Pfizer Global Research and Development, Groton, Connecticut 06340 [E. G. B., L. R. P., A. M. K. R., E. E., P. E. M., B. P. B., E. D. C., J. P. J., J. C. K., Z. L., J. D. M.] and OSI Pharmaceuticals, Uniondale, New York 11553 [K. K. I., K. P.]

ABSTRACT

Aberrant expression or activity of epidermal growth factor receptor (EGFr) or the closely related $p185^{erbB2}$ can promote cell proliferation and survival and thereby contribute to tumorigenesis. Specific antibodies and low molecular-weight tyrosine kinase inhibitors of both proteins are in clinical trials for cancer treatment. CP-654577 is a potent inhibitor selective for $p185^{erbB2}$, relative to EGFr tyrosine kinase, and selectively reduces erbB2 autophosphorylation in intact cells. Treatment of SKBr3 human breast cancer cells with CP-654577 reduces the levels of the activated form of mitogen-activated protein kinase, increases the levels of cyclin-dependent kinase inhibitor $p27^{kip1}$ and reduces expression of cyclins D and E. These biochemical changes result in a reduced level of phosphorylated retinoblastoma protein and an inhibition of cell-cycle progression at G_1. Apoptosis is triggered in both SKBr3 and another high erbB2-expressing cell line, BT474, by exposure to 1 μM CP-654577, but this effect is not observed in MCF7 cells that express low erbB2. Levels of activated Akt, an important positive regulator of cell survival, are reduced within 2 h of exposure to 250 nM CP-654577, and this may contribute to the increased apoptosis. These biochemical effects are distinct from those produced by Tarceva, a selective EGFr inhibitor. The antitumor activity of CP-654577 was investigated in athymic mice bearing s.c. tumors from Fischer rat embryo fibroblasts transfected with erbB2. CP-654577 produced a dose-dependent reduction of $p185^{erbB2}$ autophosphorylation and inhibited the growth of these tumors. CP-654577 warrants further evaluation in tumors with high expression of $p185^{erbB2}$ and may differ from selective EGFr inhibitors or nonselective dual EGFr/erbB2 inhibitors in efficacy and therapeutic index.

INTRODUCTION

The EGF[2] receptor family consists of four members (EGFr, erbB2, erbB3, and erbB4) that respond to activating ligands by homo- and heterodimerization, activation of tyrosine kinase activity, and signaling through a complex and extensively studied network of downstream effectors (1–3). Over-expression or inappropriate activation of erbB2 and EGFr have been implicated in the dysregulated growth of a wide variety of human tumors (2, 4), and this, in turn, has triggered extensive efforts to identify inhibitors of EGFr or erbB2 for use as antitumor agents (4–6).

The most advanced agent targeting these receptors is trastuzumab (Herceptin) a humanized monoclonal antibody directed against $p185^{erbB2}$. Trastuzumab has activity in breast cancer as a single agent and in combination with paclitaxel and was recently approved for the treatment of breast cancer (7–9). An antibody, cetuximab (previously C225), directed against the EGFr is also in clinical trial, and encouraging initial results have been reported (6, 10). Specific low molecular-weight reversible inhibitors of the EGFr tyrosine kinase have advanced to clinical trial (11), including Tarceva (previously designated CP-358774, erlotinib, or OSI-774; see Refs. 12–14) and gefitinib (previously designated ZD-1839 or Iressa; see Refs. 15–17). Irreversible inhibitors of EGFr and erbB2 kinase have also entered the clinic (18, 19).

The SKBr3 human breast cancer cell line expresses high levels of $p185^{erbB2}$, and proliferation of these cells is inhibited by disruption of erbB2 signals by specific antibodies, antisense oligonucleotides, or trapping of $p185^{erbB2}$ by expression of an intracellular antibody (20–23). We have recently identified a novel low molecular-weight inhibitor of $p185^{erbB2}$ kinase, with selectivity for that kinase relative to the closely related EGFr tyrosine kinase, and report here the biochemical and biological effects of that agent on breast cancer cells.

MATERIALS AND METHODS

Inhibitors and Growth Factors. CP-654577 (Fig. 1) was prepared by previously published methods (24). Tarceva was prepared as described (12). Recombinant HRG (EGF domain) was purchased from R&D Systems (Minneapolis, MN), and human recombinant EGF was from Sigma Chemical Co. (St. Louis, MO).

Cells. SKBr3, BT474, and MCF7 cells were obtained from the American Type Culture Collection (Rockville, MD). The NIH 3T3 fibroblasts transfected with chimeric EGFr/erbB2 (25) were provided by Dr. Oreste Segatto, (Istituto Regina Elena, Rome, Italy). NIH 3T3 cells transfected with human EGFr were reported previously (26). FRE-erbB2 cells were generated by transfection of Fischer rat embryo fibroblasts with human erbB2 with an activating mutation in the transmembrane region (V664E) under the control of a cytomegalovirus promoter. This plasmid was cotransfected with pRSV/Neo and pSV2/DHFR for selection and amplification. BT474 cells are grown in RPMI with 2 mM L-glutamine, 1.5 g/L sodium bicarbonate; 4.5 g/L glucose, 10 mM HEPES, 1 mM sodium pyruvate, 0.01 mg/ml bovine insulin, and 10% FBS. SKBr3 cells were grown in McCoy's 5A medium with 1.5 mM L-glutamine, 10% FBS. 3T3 and FRE-erbB2 cells were grown in DMEM with high glucose, 1.5 mM L-glutamine, and 10% FBS.

Kinase Assays. The erbB2 and EGFr kinase reactions were performed in a modified form of a previously reported assay (12). Recombinant erbB2 (amino acid residues 675-1255) and EGFr (amino acid residues 668-1211) intracellular domains were expressed in baculovirus-infected Sf9 cells as glutathione *S*-transferase fusion proteins. The proteins were purified by affinity chromatography on glutathione Sepharose beads for use in the assay. Nunc MaxiSorp 96-well plates were coated by incubation overnight at 37°C with 100 μl/well of 0.25 mg/ml poly(Glu:Tyr, 4:1), (PGT; Sigma Chemical Co.) in PBS. Excess PGT was removed by aspiration and the plate was washed 3 times with wash buffer (0.1% Tween 20 in PBS). The kinase reaction was performed in 50 μl of 50 mM HEPES (pH 7.4) containing 125 mM sodium chloride, 10 mM magnesium chloride, 0.1 mM sodium orthovanadate, 1 mM ATP, and ~15 ng of recombinant protein. Inhibitors in DMSO were added; the final DMSO concentration was 2.5%. Phosphorylation was initiated by addition of ATP and proceeded for 6 min at room temperature, with constant shaking. The kinase reaction was terminated by aspiration of the reaction mixture and washing four times with wash buffer. Phosphorylated PGT was measured after a 25-min incubation with 50 μl/well HRP conjugated-PY54 (Oncogene Science Inc. Pharmaceuticals, Uniondale, NY) antiphosphotyrosine antibody, diluted to 0.2

Received 11/25/02; accepted 6/2/03.

The costs of publication of this article were defrayed in part by the payment of page charges. This article must therefore be hereby marked *advertisement* in accordance with 18 U.S.C. Section 1734 solely to indicate this fact.

[1] To whom requests for reprints should be addressed, at Pfizer Global Research and Development, Eastern Point Rd., Groton, CT 06340. E-mail: james_d_moyer@groton.pfizer.com.

[2] The abbreviations used are: EGF, epidermal growth factor; EGFr, epidermal growth factor receptor; HRG, heregulin-β1; FBS, fetal bovine serum; PGT, ml poly(Glu:Tyr, 4:1); HRP, horseradish peroxidase; PI, propidium iodide; MAPK, mitogen-activated protein kinase; Rb, retinoblastoma.

Downloaded from http://aacrjournals.org/cancerres/article-pdf/63/15/4450/2505431/ch1503004450.pdf by guest on 22 June 2024

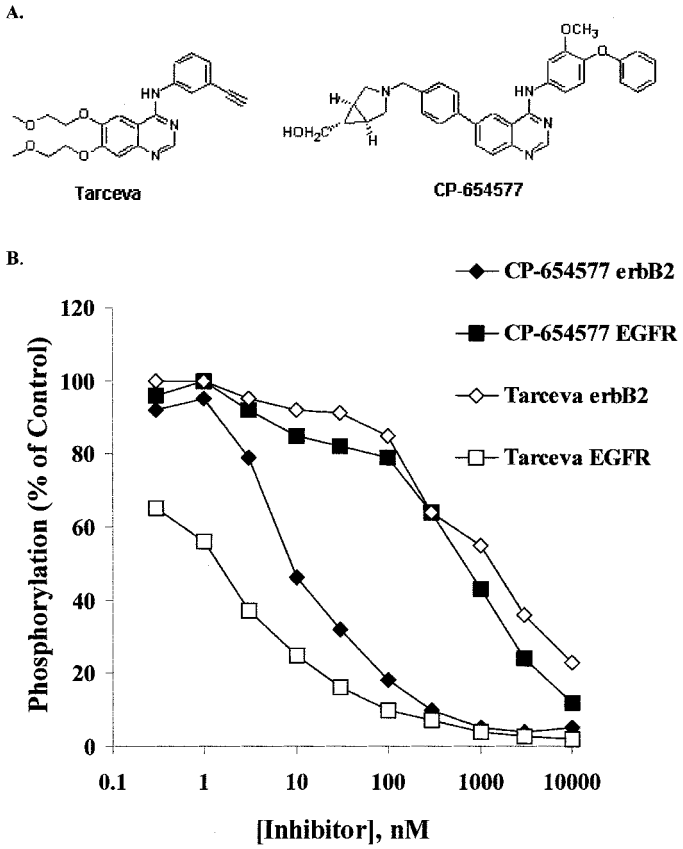

Fig. 1. Selective Inhibition of *erb*B2 Kinase. *A*, the structures of selective EGFr and *erb*B2 kinase inhibitors used in these studies. *B*, phosphorylation of poly-GluTyr by purified *erb*B2 and EGFr intracellular domains was measured by immunoassay with anti-phosphotyrosine antibodies as described in "Materials and Methods." CP-654577 inhibition of *erb*B2 (◆) and EGFr (■); Tarceva inhibition of *erb*B2 (◇) and EGFr (□). Data points are means of two determinations from a single experiment and this study was repeated twice with similar results.

μg/ml in blocking buffer (3% BSA, 0.05% Tween 20 in PBS). Antibody was removed by aspiration and the plate washed four times with wash buffer. The colorimetric signal was developed by addition of 50 μl/well Tetramethylbenzidine Microwell Peroxidase Substrate (Kirkegaard and Perry Labs, Gaithersburg, MD) and stopped by the addition of 50 μl/well 0.09 M sulfuric acid. The phosphotyrosine product formed was estimated by measurement of absorbance at 450 nm. The signal for controls was typically $A_{0.6-1.2}$, with essentially no background in wells without ATP, kinase protein, or PGT, and was proportional to the time of incubation for 6 min.

Cell Proliferation Studies. SKBr3 cells cultured in McCoys 5 A medium with 10% FBS and 1% Penn-strep + L-glutamine were seeded at 10,000 cells/well on 96-well tissue culture plates, and, 24 h later, cells were treated as indicated for an additional 24 h. Cell proliferation was estimated using the Biotrak Cell Proliferation ELISA System (Amersham Pharmacia Biotech, Arlington Heights, IL), following the manufacturer's protocol with a 3-h labeling period with the BrdUrd analogue at 37°C.

Cell Cycle Analysis. Flow cytometric analysis was done using the ABSOLUTE-S Kit (PharMingen, San Diego, CA) per the manufacturer's instructions. This is a two color staining method for measuring cell cycle distribution by analysis of DNA replication using BrdUrd incorporation and cellular DNA content/cell by PI staining.

Measurements of Total Tyrosine Protein Phosphorylation in Cells. NIH3T3 cells transfected with either human EGFr (26) or a chimeric receptor with EGFr extracellular domain and erbB2 intracellular domain (25) were seeded in 96-well tissue culture plates in DMEM. Inhibitors in DMSO (or DMSO vehicle for controls) were added 24 h after plating and incubated with the cells for 2 h at 37°C. Cells were stimulated with human recombinant EGF (50 ng/ml final concentration) for 15 min at room temperature. The medium was aspirated, and cells were fixed for 30 min with 100 μl cold 1:1 ethanol: acetone containing 200 μM sodium orthovanadate. Plates were washed with wash buffer (0.5% Tween 20 in PBS), and 100 μl of block buffer (3% BSA in PBS + 200 μM fresh sodium orthovanadate) were added. Plates were further incubated for 1 h at room temperature and washed twice with wash buffer. Antiphosphotyrosine antibody (PY54) labeled with HRP was added to wells and incubated for 1 h at room temperature. Antibody was removed by aspiration, and plates were washed 4 times with wash buffer. The colorimetric signal was developed by addition of Tetramethylbenzidine Microwell Peroxidase Substrate (Kirkegaard and Perry Labs), 50 μl/well, and stopped by the addition of 0.09 M sulfuric acid, 50 μl/well. Phosphotyrosine was estimated by measurement of absorbance at 450 nm. The signal from control wells containing no compound stimulated with EGF after subtraction of the background from wells without EGF was defined as 100% of control. EGF increased total phosphotyrosine levels by 4.3-fold in EGFr-transfected cells and 4.6-fold in erbB2/EGFr chimera transfected cells.

Western Blotting. SKBr3 cells were seeded in 24-well tissue culture plates at a density of 100,000 cells/well (MAPK, Akt, cyclin D2 and D3) or 12-well plates (p-Tyr, $p27^{kip1}$, Rb, cyclin E). After 24 h for cell attachment, compound was added to the wells as indicated. After incubation with compound, appropriate wells were stimulated with 10 ng/ml HRG or EGF for 5 min or unstimulated (basal). The concentrations and duration of stimulation were determined to provide maximal activation in a previous experiment. After stimulation, media were aspirated and 150 μl of boiling Laemmli buffer (125 mM Tris, pH 6.8; 4% SDS, 20% Glycerol, 0.6 mM $NaVO_4$) were added to wells to lyse the cells. Lysates were collected and boiled for 10 min. Cellular protein was determined using the bicinchoninic acid protein assay method (Pierce, Rockford, IL) according to the manufacturer's instructions. Equal amounts of total protein (10–20 μg) were loaded onto Bis-Tris gels for SDS-PAGE Western Blot electrophoresis and transferred to a polyvinylidene difluoride membrane. After transfer, membranes were blocked for 1 h at room temperature in either Roche Western Blocking Reagent (1921673; Indianapolis, IN) or 5% BSA in Tris-buffered saline (Sigma Chemical Co.), 0.1% Tween 20, or Blotto (4% dry milk in Tris Buffered Saline with 0.05% Tween 20, pH 8.0 (Sigma Chemical Co.) and incubated overnight at 4°C with antibodies specific for phospho-MAPK (phospho- $p42^{erk2}$ and phospho-$p44^{erk1}$ 442705; Calbiochem, San Diego, CA), MAPK (sc-94; Santa Cruz Biotechnology, Santa Cruz, CA), PhosphoPlus Akt Ser473 (9270; Cell Signaling Technology, Beverly, MA), $p27^{kip1}$ (Clone 57; BD Transduction Laboratories, Lexington, KY), Rb (G3–245; BD PharMingen), cyclin D2 C-17 (sc-181; Santa Cruz Biotechnology), cyclin D3 C-16 (sc-182; Santa Cruz Biotechnology) phosphotyrosine (PY54-HRP; OSIP, Nassau, NY) or cyclin E (Clone HE12; BD PharMingen, San Diego, CA). After washing with Tris Buffered Saline with 0.05% Tween 20, pH 8.0 (Sigma Chemical Co.), the membranes were incubated with antimouse or antirabbit HRP-conjugated secondary antibodies (554002; BD PharMingen, San Diego, CA; NA931; Amersham, IL; 554021; BD PharMingen; sc-2004; Santa Cruz Biotechnology; Cell Signaling Technology) for 1 h at room temperature, washed again, and developed by enhanced chemiluminescence according to the manufacturer's instructions (ECL; Amersham Pharmacia Biotech, Piscataway, NJ; LumiGLO; Cell Signaling Technology) and quantitated by densitometry using a Kodak Image Station 440CF.

Analysis of erbB Phosphorylation by Immunoprecipitation Followed by Western Blotting. SKBr3 cells were treated with compound at the indicated concentrate for 2 h before stimulation. The media were aspirated, and 1 ml/75 cm^2 flask ice-cold immunoprecipitation lysis buffer [1.0% Triton X-100; 10 mM Tris; 5 mM EDTA; 50 mM NaCl; 30 mM $Na_4P_2O_7$ with freshly added 100 μM Na_3VaO_4; 100 μM PMSF; and one Complete protease inhibitor tablet (Roche Diagnostics, Indianapolis, IN)/50 ml buffer] was added. Immunoprecipitation was performed on 100 μl of lysate: EGFr was immunoprecipitated using Santa Cruz SC-120 (Santa Cruz Biotechnology), 2 μg/100 μl lysate; erbB2 using Oncogene OP15 (Oncogene Science Inc. Pharmaceuticals), 1 μg/100 μl lysate; and erbB3 with Santa Cruz SC-285 (Santa Cruz Biotechnology), 2 μg/100 μl lysate. All immunoprecipitations were carried out at 4°C overnight, with rocking, in the presence of 30 μl of protein A beads. The beads with immobilized protein were isolated by centrifugation at 14,000 rpm at 4°C for 10 s. The supernatants were aspirated and the pellets washed three times with PBS with 0.1% Tween 20. The samples were then resuspended in 40 μl of Laemmli buffer with DTT and boiled for 4 min. The samples were then loaded on a 4–12% PAGE. They were electrophoresed 1 h at 150 V using 2[N-morpholino]ethanesulfonic acid buffer. The gels were transferred to poly-

Downloaded from http://aacrjournals.org/cancerres/article-pdf/63/15/4450/2505431/ch1503004450.pdf by guest on 22 June 2024

vinylidene difluoride in the presence of 10% methanol. The membrane was blocked using blocking buffer (Roche Diagnostics), and the phosphotyrosine signal was detected using anti-PY54 antibody conjugated to HRP. Chemiluminescence signal was generated with Amersham ECL reagents and quantitated with a Lumi-imager (Roche Molecular Biochemicals, Indianapolis, IN).

Measurements of Apoptosis. BT474, SKBr3, and MCF7 cells were seeded in cell culture medium containing 10% FBS in 4-well (60 mm) plates. The next day the medium was replaced with fresh medium containing 0.5% FBS and the vehicle (DMSO), CP-654577, or staurosporine (positive control). Cells were incubated for 48 h at 37°C. Both adherent and nonadherent cells were harvested and analyzed for apoptosis. Phosphatidylserine externalization was measured using the ApoAlert Annexin V-FITC kit (Clontech, Palo Alto, CA). Cells were labeled with annexin V-FITC and counterstained with PI per the kit instructions. Disruption of the mitochondrial membrane potential ($\Delta\Psi$m) was measured using the DePsipher Kit (Trevigen, Gaithersburg, MD) according to the kit instructions. Valinomycin- and staurosporine-treated cells were used as positive controls. Caspase activation was measured using the CaspaTag Fluorescein Caspase (VAD) Assay Kit (Intergen, Purchase, NY) according to the kit instructions. Staurosporine-treated cells were used as a positive control. DNA fragmentation was measured by terminal deoxynucleotidyltransferase dUTP nick end labeling using the APO-BRDU Kit (PharMingen, San Diego, CA). Positive and negative control cells supplied with the kit were analyzed in parallel with samples. For all four assays, binding of fluorescent probes was measured on a FACSCalibur flow cytometer (Becton Dickinson, San Jose, CA) equipped with a 488-nm argon laser. FITC and carboxyfluorescein were detected in the FL1 channel, PI in the FL2 channel, and JC-1 in FL1 and FL2 channels. Data were analyzed using CellQuest software.

Determination of Tumor Xenograft erbB2 Phosphorylation and Tumor Growth Inhibition. Three to 4-week-old female athymic mice (CD-1 Nu/Nu) were used for tumor xenografts. Mice were obtained from Charles River Laboratories (Wilmington, MA) and were housed in specific pathogen-free conditions, according to the guidelines of the Association for Assessment and Accreditation of Laboratory Animal Care (27); all studies were carried out under approved institutional experimental animal care and use protocols. During these studies, animals were provided pelleted food and water *ad libitum* and kept in a room conditioned at 70–75°F and 50- 60% relative humidity with >15 fresh air changes per hour. Sentinel mice were monitored routinely at 4-week intervals by serological assays and were found to be free of exposure to the following agents: murine hepatitis virus, Sendai virus, pneumonia virus of mice, Minute virus of mice, mouse poliovirus, type 3 reovirus, *Mycoplasma pulmonis*, mouse parvovirus, and epizootic diarrhea of infant mice. In addition, the sentinels were monitored on a quarterly basis for lymphocytic choriomeningitis virus, mouse adenovirus, ectromelia, mouse pneumonitis, and polyomavirus. For all studies, the mice were allowed to acclimate 3 days after receipt of shipment; test animals were randomized before commencement of treatments.

For determination of erbB2 tyrosine phosphorylation, tumors were isolated 2 hours postdose and homogenized in ice-cold lysis buffer [50 mM HEPES (pH 7.4)/150 mM NaCl/1.5 mM $MgCl_2$/1 mM EDTA/1% Glycerol/1% Triton X-100/1.6 mM Na_3VO_4/50 mM NaF/Protease Inhibitor Cocktail (catalog number 1873580; Boehringer Mannheim, Germany) at 1 ml buffer/100 mg tumor wet weight]. ErbB2 phosphorylation status was determined using a neu ELISA Kit (Oncogene Research Products, Boston, MA) to capture the receptor and the plate is probed with an HRP-conjugated anti-phosphotyrosine antibody (PY54). Inhibition of erbB2 phosphorylation was measured as the decrease of ELISA signal relative to the vehicle-treated control tumors.

For the tumor growth inhibition study, 10 days after inoculation animals bearing tumors of ~150 mm^3 in size were divided into four groups. CP-654577 was formulated in 5% Gelucire (44/14; Gattefosse Inc., Saint Priest Cedex, France)/95% sterile water and dosed at 12.5, 25, and 50 mg/kg or with vehicle twice daily, i.p. injection. Animal body weight and tumor measurements (mm) were obtained every 2 to 3 days. Tumor volume (mm^3) was calculated using the formula: length (mm) × width (mm) × width (mm) × 0.5.

RESULTS

Selective Inhibition of erbB2 Kinase by CP-654577. The inhibitors characterized in this report share a 4-anilino-quinazoline as a core structure (Fig. 1*A*), but differ greatly in their selectivity for the inhibition of the highly homologous EGFr and erbB2 tyrosine kinases. Tarceva is a selective inhibitor of the EGFr tyrosine kinase (12) with greatly reduced potency as an inhibitor of erbB2 tyrosine kinase (Fig. 1*B*). In contrast, the novel compound CP-654577 selectively inhibits the kinase activity of erbB2 as measured by phosphorylation of immobilized poly glutamic acid tyrosine copolymer (IC_{50}, 11 nM) and is 60-fold less potent (IC_{50}, 670 nM) as an inhibitor of EGFr tyrosine kinase (Fig. 1*B*). CP-654577 was also evaluated as an inhibitor of purified human c-src kinase, recombinant insulin receptor kinase, recombinant insulin-like growth factor receptor kinase, and recombinant platelet derived growth-factor receptor kinase (data not shown). Although some inhibition was noted for each kinase at higher concentrations of inhibitor, the IC_{50} values were >5 μM, except for c-src (IC_{50} = 1.8 μM). Thus, the previously reported selectivity of aminoquinazolines for erbB family kinases is maintained in this compound (12, 17).

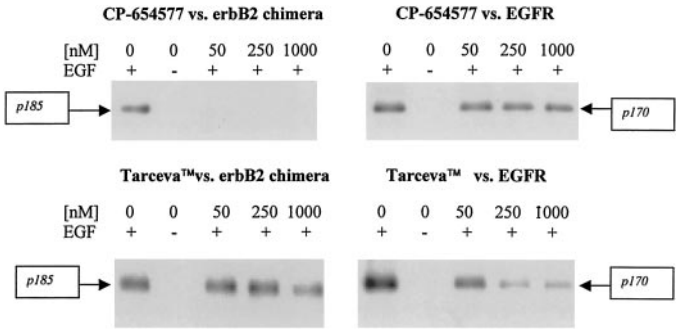

Fig. 2. CP-654577 Selectively Inhibits *erb*B2 Kinase in Intact Cells. Murine 3T3 fibroblasts transfected with either an EGFr/*erb*B2 chimera or EGFr were pretreated with the indicated concentration of inhibitors for 2 h, then EGF (50 ng/ml) was added as indicated. After 15 min of stimulation at room temperature, lysates were prepared and analyzed for phosphorylated receptor by Western blot with an antiphosphotyrosine antibody as described in "Materials and Methods." This result is representative of three independent experiments.

This pattern of selective inhibition by these two compounds is recapitulated in intact cells. Murine 3T3 cells transfected either with human EGFr (26) or with a chimeric receptor consisting of the extracellular domain of EGFr coupled with the intracellular domain (including the tyrosine kinase domain) of erbB2 (25) were used for these studies. Each of these cell lines respond to the addition of EGF with robust autophosphorylation of the transfected receptor, representing EGFr or erbB2 tyrosine kinase respectively (Fig. 2). CP-645577 at concentrations as low as 50 nM blocks erbB2 activity, but only produces a modest inhibition of EGFr activity at 1 μM. Conversely, Tarceva reduces EGFr phosphorylation at 50 nM and has only modest effects on erbB2 activity at 1 μM. As an alternative more quantitative approach, we examined the potency of the compounds in the inhibition of EGF-induced total phosphotyrosine of the transfected cells (Table 1). Again, CP-654577 was much more potent at suppressing the erbB2 chimera than EGFr, whereas Tarceva had the opposite pattern, *i.e.*, it inhibited EGFr more potently than the erbB2 chimera. Therefore, the pattern of selectivity seen in the kinase assay was also observed in the intact cell assay.

Inhibition of erbB Tyrosine Phosphorylation in SKBr3 Cells. SKBr3 cells express very high levels of erbB2, elevated levels of EGFr and lower levels of erbB3 (27, 28). In these cells, erbB proteins of ~170–185 kDa are constitutively phosphorylated on tyrosine residues. Examination of erbB protein phosphorylation of SKBr3 cells by Western blotting as described in "Materials and Methods" indicated that addition of CP-654577 to cells in culture leads to a rapid concentration-dependent reduction of this erbB tyrosine phosphorylation.

Downloaded from http://aacrjournals.org/cancerres/article-pdf/63/15/4450/2505431/ch1503004450.pdf by guest on 22 June 2024

Table 1 *Inhibition of EGF-induced tyrosine phosphorylation in transfected 3T3 cells*

EGF-stimulated phosphotyrosine content was evaluated after a 15-min stimulation with 50 ng/ml EGF to the indicated cell line as described in "Materials and Methods." Inhibitors at the indicated concentrations were pre-incubated with the cells for 2 h prior to stimulation. Mean ± SD is indicated for quadruplicate determinations.

		Phosphotyrosine content % of EGF-stimulated control	
Inhibitor	Concentration (μM)	EGFr transfectant	ErbB2/EGFr chimera transfectant
None (Control)	(DMSO vehicle)	100 ± 4	100 ± 3
Tarceva	0.1	31 ± 0.5	89 ± 2
Tarceva	0.3	20 ± 0.4	74 ± 2
Tarceva	1	7 ± 0.5	46 ± 2
Tarceva	3	<5	7 ± 5
CP-654577	0.1	101 ± 1	23 ± 0.5
CP-654577	0.3	74 ± 6	6 ± 1
CP-654577	1	31 ± 12	<5
CP-654577	3	14 ± 2	<5

This effect is apparent at CP-654577 concentrations as low as 50 nM within 4 h of exposure (~50%), depletion was >75% at 1000 nM, and persisted for 24 h (blots not shown).

To explore in detail the effects of these selective inhibitors on receptor phosphorylation, the tyrosine phosphorylation status of EGFr, erbB2, and erbB3 of SKBr3 cells were evaluated individually after inhibitor treatment (Fig. 3). These experiments were conducted on cells without addition of ligand and also in cells stimulated by the addition of the EGFr activating ligand EGF and the erbB3 ligand HRG. The levels of tyrosine phosphorylation of all three receptors were measured by Western blotting with anti-phosphotyrosine antibodies after specific immunoprecipitation. In SKBr3 cells, stimulation with EGF produces the most dramatic change: a 17-fold increase in EGFr receptor phosphorylation, a modest increase in erbB2 phosphorylation, and essentially no change in erbB3 phosphorylation (Fig. 3*A*). HRG produces a 3.9-fold increase in erbB3 phosphorylation and slight reduction in EGFr and erbB2 phosphorylation.

In unstimulated SKBr3 cells, both Tarceva and CP-654577 produced a concentration-dependent reduction in EGFr tyrosine phosphorylation (Fig. 3*B*), but the erbB2-selective inhibitor CP-654577 was much more potent at reducing erbB2 and erbB3 tyrosine phosphorylation. Despite its superior potency for reduction of erbB2 phosphorylation relative to Tarceva, CP-654577 also produced a significant depletion of EGFr phosphorylation in these cells (Fig. 3*B*), presumably because of inhibition of the transphosphorylation of EGFr by erbB2 in heterodimers. Both inhibitors reduced EGFr phosphorylation in heregulin-stimulated cells in a concentration dependent fashion (Fig. 3*C*). Tarceva was ineffective at reducing erbB2 phosphorylation in HRG-stimulated cells, whereas CP-654577 produced a potent concentration-dependent reduction. The two inhibitors were similarly effective in reduction of HRG-stimulated erbB3 phosphorylation. In contrast, the EGFr-selective inhibitor Tarceva was strikingly more potent than CP-654577 in reducing EGFr phosphorylation in EGF-stimulated cells (Fig. 3*D*), although CP-654577 also produced a concentration-dependent reduction in EGFr phosphorylation. This effect of CP-654577 may result from either inhibition of erbB2-kinase dependent EGFr phosphorylation in EGFr/erbB2 heterodimers, or from the incomplete specificity of CP-654577 for erbB2 kinase. Tarceva reduced both erbB2 and erbB3 phosphorylation in EGF-stimulated cells to a similar extent at all three concentrations tested, whereas CP-654577 was less potent but reduced EGF-stimulated

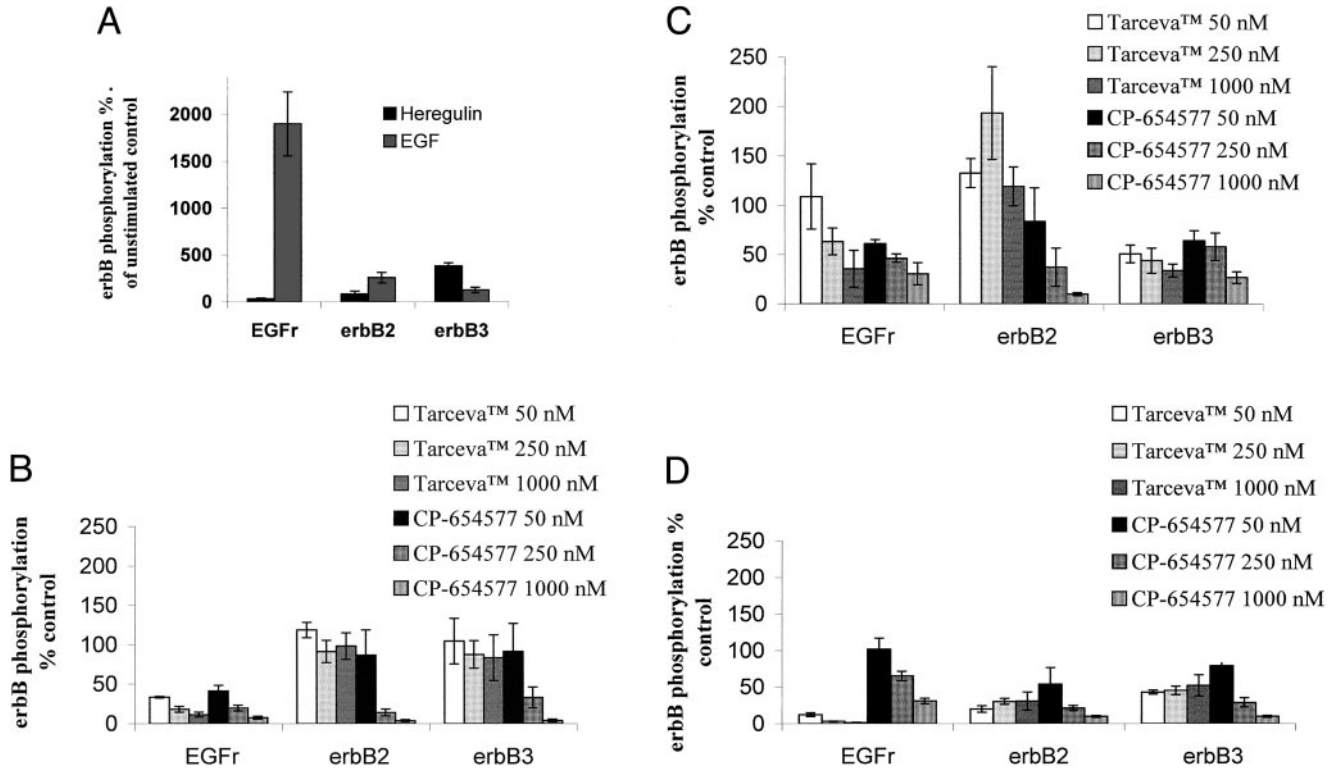

Fig. 3. Effect of Selective Inhibitors on EGF, *erb*B2, and erbB3 Receptor Phosphorylation in SKBr3 Cells. SKBr3 cells were treated with Tarceva or CP-654577 for 2 h. Cells were stimulated for 5 min by addition of 10 ng/ml EGF or HRG to the medium or unstimulated (basal) as indicated. The indicated receptors were isolated by immunoprecipitation and tyrosine phosphorylation was estimated by Western blotting with antiphosphotyrosine antibodies as described in "Materials and Methods." The combined results of two experiments are shown (mean ± SE, $n = 4$). To show relative levels of stimulation, phosphotyrosine signal from each receptor type was compared with the phosphotyrosine signal of the appropriate control as indicated. *A*, basal phosphotyrosine signal of immunoprecipitated EGFr, erbB2, and erbB3 from cells treated with compound were compared with receptors immunoprecipitated from untreated cells. (*B*). Inhibitor effect on receptor tyrosine phosphorylation in unstimulated (basal) cells relative to untreated control cells. *C*, inhibitor effect on receptor phosphotyrosine of heregulin-treated cells relative to heregulin-treated control cells. *D*, inhibitor effect on receptor phosphotyrosine of EGF-treated cells relative to EGF-treated control cells.

Downloaded from http://aacrjournals.org/cancerres/article-pdf/63/15/4450/2505431/ch1503004450.pdf by guest on 22 June 2024

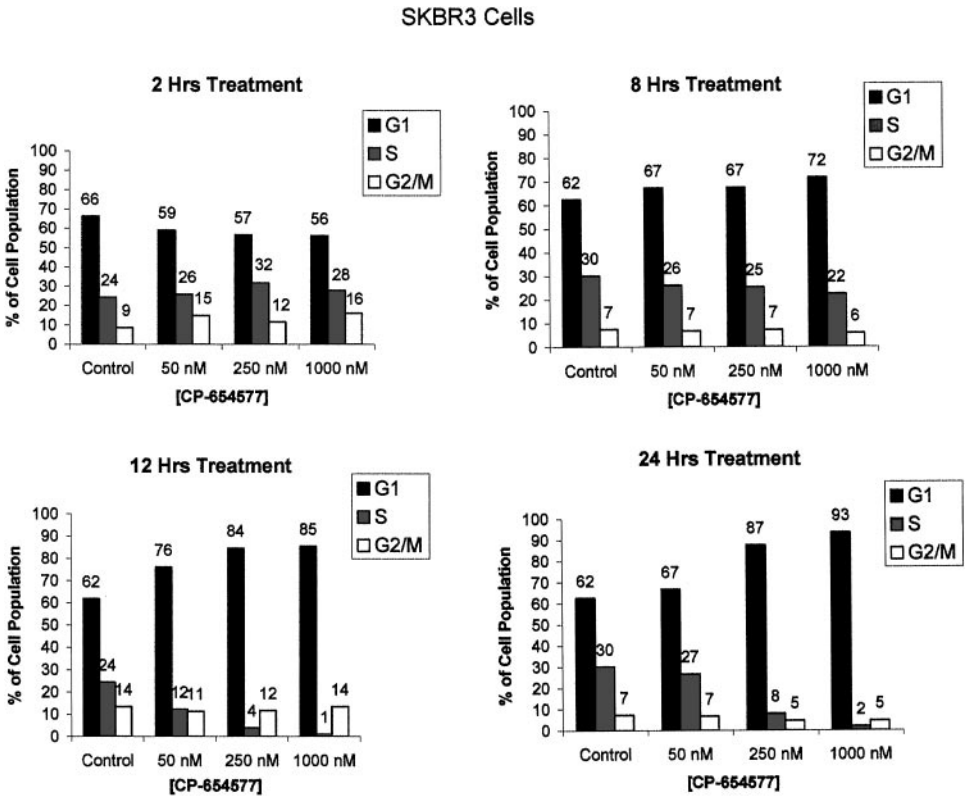

Fig. 4. Analysis of the cell cycle distribution after treatment of SKBr3 cells with CP-654577. SKBr3 cells were treated as indicated and cell cycle analyzed by flow cytometry as described in "Materials and Methods." The *numbers* over each *bar* indicate the percentage of cells in that phase of the cell cycle. This pattern was observed in three independent experiments.

erbB2 and erbB3 phosphorylation in a concentration-dependent manner and to a greater extent than Tarceva at the highest concentration.

The overall pattern of inhibition observed is complex, but consistent with the selectivity pattern indicated by the kinase and 3T3 cell results. Tarceva is a much more potent inhibitor of EGF-induced EGFr phosphorylation, whereas CP-654577 is more potent in reduction of basal erbB2 and erbB3 phosphorylation.

Effect of erbB2 Inhibition on Cell Proliferation. CP-654577 inhibits SKBr3 cell proliferation after 24-h exposure as measured by bromodeoxyuridine incorporation (see "Materials and Methods") with an IC_{50} of 55 ± 20 nM (mean ± SE, $n = 5$ independent experiments), whereas the EGFr-selective inhibitor Tarceva was much less potent: IC_{50s} of 800 nM and >1000 nM were observed in two independent titrations. To better characterize this antiproliferative effect, we examined the effect of CP-654577 on SKBr3 cell cycle distribution (Fig. 4). No change in SKBr3 cell cycle phase distribution was seen after a 2-h treatment with CP-654577, but after 12 h, the G_1 cell population increased from 62% to 84% in cells treated with 250 nM CP-654577. Cells in S phase decreased from 24% to 4%, with no change in the percent of cells in G_2/M phase. The cell-cycle effects were concentration-dependent, with marked and sustained effects at 250 nM and 1 μM. Thus a G_1 cell-cycle arrest is rapidly produced by inhibition of the erbB2 receptor in SKBr3 cells treated with CP-654577.

Biochemical Basis of the Cell Cycle Blockade. To evaluate the basis of the CP-654577-induced cell-cycle block, we examined some of the key mediators of erbB2 signal transduction and cell cycle regulation. The phosphorylation of Rb protein regulates the G_1 to S-phase transition at the restriction point and is tightly controlled by cyclin/cdk complexes, particularly the cyclin D/cdk4 and cyclin E/cdk2 complexes (29). SKBr3 cells normally contain primarily phosphorylated Rb protein (Fig. 5*A*, *upper band*), but SKBr3 cells treated with CP-654577 showed a gradual loss of the more highly phosphorylated (ppRb) form and a corresponding increase in the lower hypophosphorylated form (pRb) after a 4-h treatment (Fig. 5*A*). At 24-h exposure to 1 μM CP-654577, the ppRb form is virtually absent: >88% reduced by densitometric analysis of the autoradiograms. These observations are consistent with the ability of CP-654577 to arrest SKBr3 cells in the G_1 phase.

Several effects of CP-654577 on proteins that regulate Rb phosphorylation were observed. A key regulator of cyclin dependent kinase and entry into S phase is $p27^{kip1}$, an inhibitor of cdk2. Inhibition of the erbB2 receptor by CP-654577 (250 nM) induces ~3-fold $p27^{kip1}$ protein accumulation by 12 h of treatment as estimated by densitometry (Fig. 5*B*). Cyclin E expression decreased within 4 h of exposure to the erbB2 inhibitor (Fig. 5*C*), with marked decreases upon 12 h exposure to 250 nM CP-654577 and nearly complete disappearance after 12 h exposure to 1 μM inhibitor. Cyclin D2 and cyclin D3 regulate the transition between phases of the cell cycle by modulating cdk activity. CP-654577 induced a decrease of 40% in cyclin D2 levels within 2 h of exposure at 250 nM and 1 μM (Fig. 5*D*). This decrease was more pronounced at 12 h at 250 nM (70% inhibition) and 1 μM (90% inhibition). Cyclin D2 levels were also depressed in the 250 nM (60% inhibition) and 1 μM (85% inhibition) groups at 24 h postdose. Our efforts to monitor changes in cyclin D3 expression were impeded by relatively low signals in Western blots (not shown). It was clear, however, that after 24 h of exposure to 250 nM or 1 μM CP-654577 cyclin D3 levels were reduced by >75%.

Comparative Evaluation of Tarceva and CP-654577 Effects on MAPK and Akt Activation. The MAPKs ERK1 and ERK2 are part of a protein kinase cascade that plays a critical role in the regulation of cell growth, survival, and differentiation, in part, through effects on cyclins and cyclin-dependent kinases (30). Phosphorylation of MAPKs at threonine 202 and tyrosine 204 activates the kinase, and antibodies to the phosphorylated form can be used to monitor the activation state of the enzyme in cell lysates. As early as 2 h after exposure to CP-654577, the level of phosphorylated MAPK was reduced in a concentration-dependent manner (Fig. 6*A*), and this reduction persisted at 12 and 24 h of exposure. The reduction of

Downloaded from http://aacrjournals.org/cancerres/article-pdf/63/15/4450/2505431/ch1503004450.pdf by guest on 22 June 2024

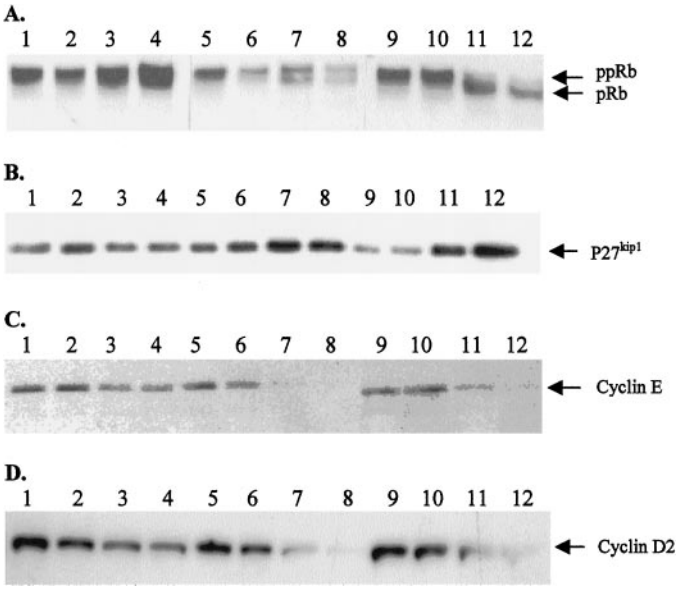

Fig. 5. Analysis of Key Cell Cycle Regulators. A, Western Blot analysis of Rb phosphorylation in SKBr3 cells after treatment with CP-654577 for 4 h (*Lanes* 2–4), 12 h (*Lanes* 6–8), 24 h (*Lanes* 10–12). Lanes 1, 5 and 9 are untreated controls. Lanes 2, 6 and 10 were treated with 50 nM. Lanes 3, 7 and 11 with 250 nM and Lanes 4, 8 and 12 with 1 μM. *B*, Western Blot Analysis of $p27^{kip1}$ in SKBr3 cells after treatment with CP-654577 for 2 h (*Lanes* 12–4), 12 h (*Lanes* 6–8) and 24 h (*Lanes* 10–12). Untreated controls are on *Lanes* 1, 5 and 9; 50 nM CP-654577, *Lanes* 2, 6 and 10; 250 nM, *Lanes* 3, 7 and 11; 1 μM, *Lanes* 4, 8 and 12. *C*, Western Blot analysis of cyclin E inhibition by CP-654577 after 4 h (*Lanes* 2–4), 12 h (*Lanes* 6–8), 24 h (*Lanes* 10–12). Lanes 1, 5 and 9 are untreated controls. Lanes 2, 6 and 10 were treated with 50 nM. Lanes 3, 7 and 11 with 250 nM and Lanes 4, 8 and 12 with 1 μM. *D*, depletion of cyclin D2 by CP-654577. Western Blot analysis of cyclin D2 in SKBr3 cells treated with CP-654577 and cyclin D2 levels measured by Western blotting. Cells were exposed to compound for 2 h (*Lanes* 2–4), 12 h (*Lanes* 6–8) and 24 h (*Lanes* 10–12) respectively. Lanes 1, 5 and 9 are untreated controls. CP-654577 concentrations were 50 nM, *Lanes* 2, 6 and 10; 250 nM, *Lanes* 3, 7 and 11; or 1 μM, *Lanes* 4, 8, and 12 respectively. All blots are representative of results seen in at least two independent experiments.

phosphorylated MAPK was most pronounced at 2 h, 70% at 50 nM CP-654577 and 90% at concentrations of 250 nM and 1 μM. By 24 h, reduction of phosphorylated MAPK was less pronounced, but was still 80% at 1 μM. In these experiments the overall level of MAPK protein was unaffected (Fig. 6*A*); thus, the effect of CP-654577 is primarily on protein activation by phosphorylation.

To further evaluate the erbB2 and EGFr selectivity of Tarceva and CP-654577 in SKBr3 cells, we treated cells with inhibitors and examined the effects on basal MAPK activation or in cells stimulated with either HRG or EGF. Stimulation of SKBr3 cells by HRG or EGF resulted in a large increase (7–10 fold by densitometric analysis) in p-MAPK (Fig. 6*B*). In nonstimulated cells (basal), erbB2 selective CP-654577 was more effective in reducing basal levels of p-MAPK than EGFr selective Tarceva (Fig. 6, *B* and *C*). CP-654577 at 50 nM reduced basal p-MAPK by 90% whereas reduction by Tarceva was 20%. CP-654577 and Tarceva were comparable in their efficacy in reduction of HRG-stimulated MAPK activation. As expected, the EGFr-selective inhibitor Tarceva effectively reduced EGF-stimulated activation of MAPK (90% inhibition at 1 μM, Fig. 6*C*), but the erbB2 selective inhibitor CP-654577 only slightly inhibited MAPK activation by EGF.

In addition to mitogenic signals, erbB proteins provide survival signals in some cells, in part by activation of the Akt kinase secondary to activation of PI-3-kinase (31–34). The activation of Akt is mediated by phosphorylation of Akt at Ser473. The activity/phosphorylation of Akt was analyzed using a phospho-specific anti-Akt antibody. SKBr3 cells have a substantial basal level of activated Akt, but CP-654577 treatment leads to transient reduction in the levels of activated Akt even at 50 nM within 2 h (Fig. 7*A*). Some reactivation of Akt occurs at later times in the presence of 50 nM inhibitor, but inactivation is sustained at higher concentrations. Activated Akt levels increase sharply upon addition of EGF or HRG (Fig. 7*B*, compare *Lanes 10* and 11 to *Lanes 1* and 5). In unstimulated cells, CP-654577 is more potent at reducing p-Akt than Tarceva (Fig. 7, *B* and *C*); the former was effective at 50 nM, the latter had no effect. As expected, Tarceva is more effective in blocking EGF-induced activation of p-Akt than CP-654577 (Fig. 7*C*).

Induction of Apoptosis by CP-654577. To further characterize the effects of erbB2 inhibition by CP-654577, we examined its effect on induction of apoptosis. As a measure of apoptotic cells, we examined externalization of plasma membrane phosphatidylserine by flow cytometry. By this measure a 48 h incubation with CP-654577 induced a concentration-dependent increase in apoptosis in the high

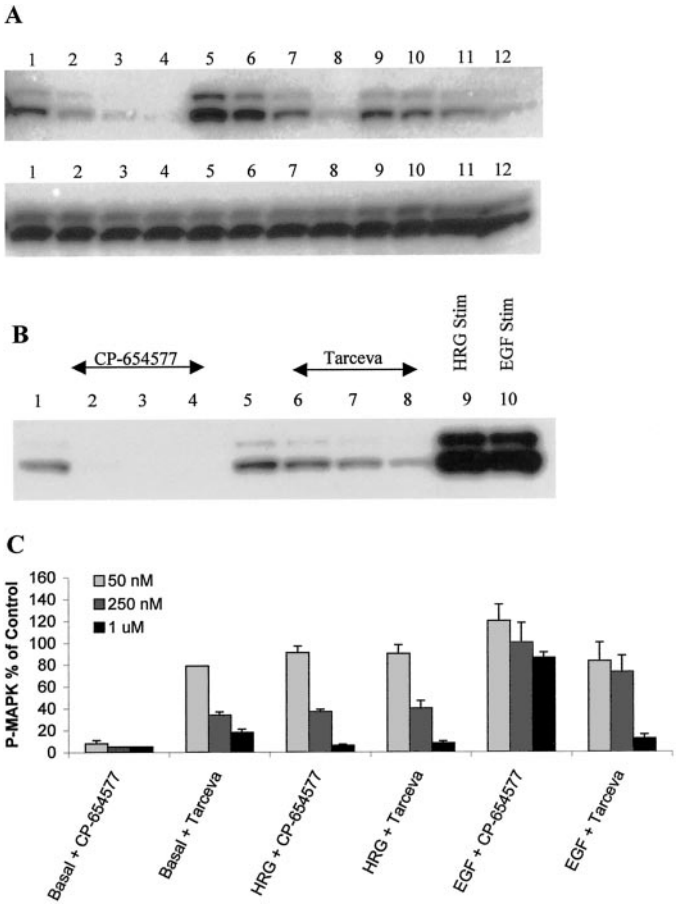

Fig. 6. Effect of erbB2 Inhibition on Activation of MAPK. For these studies, SKBr3 cells were seeded in 24-well plates at a density of 100,000 cells/well and used the next day. *A*, SKBr3 cells were untreated (*Lanes* 1, 5, and 9) or treated with CP-654577 for 2 h (*Lanes* 2–4), 12 h (*Lanes* 6–8) and 24 h (*Lanes* 10–12). CP-654577 concentrations were 50 nM, *Lanes* 2, 6, and 10; 250 nM, *Lanes* 3, 7 and 11 and 1 μM *Lanes* 4, 8, and 12 respectively. Lysates were examined for phosphorylated MAPK (upper blot) and total MAPK (lower blot) as described in Methods. *B*, inhibition of MAPK activation in unstimulated SKBr3 cells. Inhibitor was added to the wells at concentrations of 50 (*Lanes* 2 and 6), 250 (*Lanes* 3 and 7) or 1 μM (*Lanes* 4 and 8). Lanes 1 and 5 are of lysates from untreated controls. After 2 h exposure to inhibitor, cell lysates were prepared and phosphorylated MAPK in the lysates was visualized by Western blotting as described in Methods. Similarly, control cells (unexposed to inhibitor) were stimulated with 10 ng/ml HRG (*Lane* 9) or EGF (*Lane* 10) for 5 min and lysates prepared and examined. The concentrations and duration of stimulation were determined to provide maximal activation in a previous experiment. *C*, Cells were treated with the indicated concentration of inhibitors for 2 h, then either lysed immediately (Basal) or stimulated for 5 min with 10 ng/ml HRG or EGF as indicated before preparation of lysates. Phospho-MAPK content of the lysates was analyzed by Western blotting and quantitated by densitometry, relative to the corresponding controls without inhibitor as described in Materials and Methods. The mean ± SE is indicated, $n = 3$.

Downloaded from http://aacrjournals.org/cancerres/article-pdf/63/15/4450/2505431/ch1503004450.pdf by guest on 22 June 2024

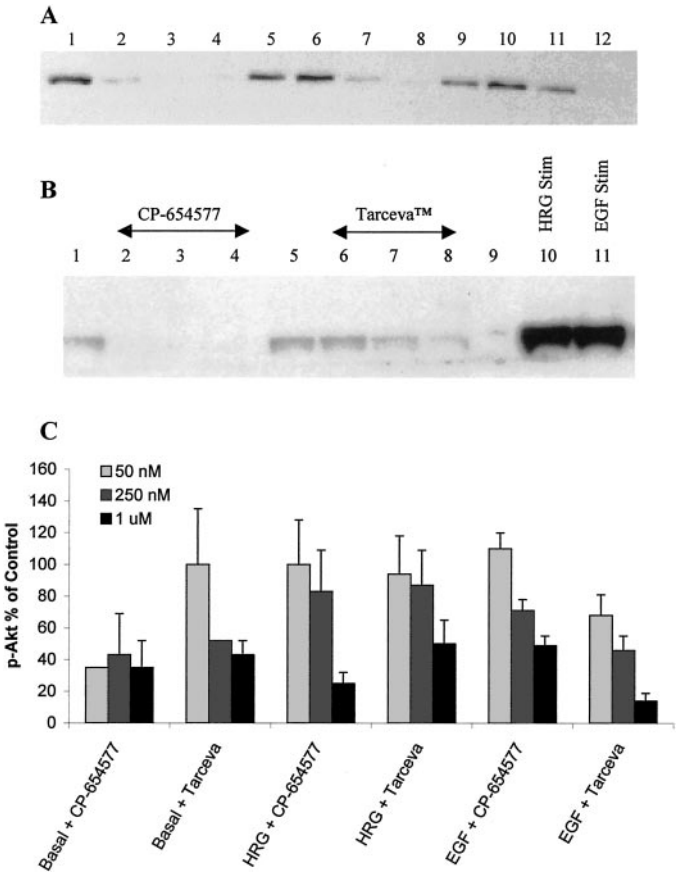

Fig. 7. CP-654577 Produces Rapid Inactivation of Akt. For these studies, SKBr3 cells were seeded in 24-well plates at a density of 100,000 cells/well and used the next day. *A*, SKBr3 cells were untreated (*Lanes* 1, 5, and 9) or treated with CP-654577 for 2 h (*Lanes* 2–4), 12 h (*Lanes* 6–8) and 24 h (*Lanes* 10–12). CP-654577 concentrations were 50 nM, *Lanes* 2, 6, and 10; 250 nM, *Lanes* 3, 7, and 11 and 1 μM *Lanes* 4, 8, and 12 respectively. Phosphorylated Akt (Ser 473) is visualized by Western blotting as described in Methods. *B*, inhibition of p-Akt in unstimulated SKBr3 cells. Inhibitor was added to the wells at concentrations of 50 nM (*Lanes* 2 and 6), 250 nM (*Lanes* 3 and 7) or 1 μM (*Lanes* 4 and 8). Lanes 1 and 5 are untreated controls. After 2 h cell lysates were prepared and phosphorylated Akt (Ser 473) was visualized by Western blotting as described in Methods. Similarly, control cells (unexposed to inhibitor) were stimulated with 10 ng/ml HRG (*Lane* 10) or EGF (*Lane* 11) for 5 min and lysates prepared and examined. The concentrations and duration of stimulation were determined to provide maximal activation in a previous experiment. *C*, cells were treated with the indicated concentration of inhibitors for 2 h, then either lysed immediately (Basal) or stimulated for 5 min with 10 ng/ml HRG or EGF as indicated. Lysates were then prepared and p-Akt was analyzed by Western blotting and quantitated by densitometry, relative to the corresponding controls without inhibitor as described in Materials and Methods. The mean ± SE is indicated, $n = 3$.

erbB2-expressing BT474 and SKBr3 cells but not in MCF7 cells which express low levels of erbB2 (Fig. 8).

As a second measure of induction of apoptosis, we examined the collapse of the mitochondrial membrane potential. By this measure, 48 h exposure to CP-654577 induced apoptosis in BT474 cells in a concentration dependent manner, but did not induce apoptosis in MCF7 cells (Table 2). The direct mitochondrial depolarization reagent valinomycin induced massive depolarization in both cell types (Table 2). Additional measures of apoptosis (DNA fragmentation measured by deoxynucleotidyltransferase dUTP nick end labeling and caspase activation) also confirmed the induction of apoptosis by CP-654577 in BT474 but not MCF7 cells (data not shown).

In summary, the pro-apoptotic effects of CP-654577 were demonstrated using four independent methods and shown to be selective for erbB2-overexpressing SKBr3 and BT474 cells, as compared with MCF7 cells, which express low levels of erbB2.

Effect of CP-654577 on Tumor Xenografts. Studies were conducted to establish whether CP-654577 could inhibit erbB2 activity and tumor growth in tumor xenografts. Unfortunately, SKBr3 cells are poorly tumorigenic in athymic mice, thus we turned to an alternative mechanistically defined model; FRE cells transformed by transfection of constitutively activated erbB2. CP-654577 treatment reduced the

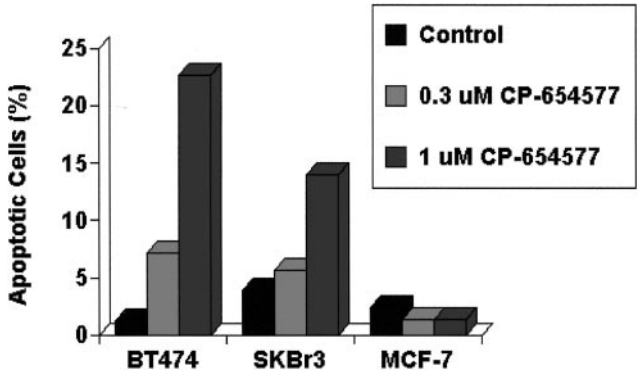

Fig. 8. Induction of Apoptosis by CP-654577. Cells were incubated with CP-654577 or vehicle for 48 h and labeled with annexin V-FITC and PI as described in "Materials and Methods." Data were acquired on a FACSCalibur flow cytometer and analyzed by dot plots of PI fluorescence (FL2) *versus* FITC fluorescence (FL1). Cells which were AV+/PI- were scored as apoptotic and are shown in the bar graph above. All determinations were performed in duplicate and the results are representative of three independent experiments.

Table 2 *Induction of Apoptosis by CP-654577*

BT474 cells or MCF7 cells in growth medium were treated as indicated for 48 h and apoptosis was estimated by depolarization of the mitochondrial membrane ($\delta\Psi$m) as described in Materials and Methods. After incubation with CP-654577 for 48 h, BT474 and MCF7 cells were stained with JC-1. Healthy and apoptotic cells were visualized simultaneously by flow cytometry using the FL2 (propidium iodide) channel to detect JC-1 red aggregates and the FL1 (fluorescein) channel to detect JC-1 green monomers. Red−/green+ cells were scored as apoptotic and were easily distinguished from non-apoptotic (red+/green+) cells. The ionophore valinomycin (100 nM) was used as a positive control and caused loss of JC-1 red fluorescence in both BT474 and MCF7 cells. Determinations were performed in duplicate and the results are representative of two independent experiments.

Cell	Treatment	% apoptotic cells
BT474	Vehicle (DMSO)	5
BT474	CP-654577 100 nM	8
BT474	CP-654577 300 nM	18
BT474	CP-654577 1000 nM	31
BT474	Valinomycin 100 nM	66
MCF7	Vehicle (DMSO)	9
MCF7	CP-654577 1000 nM	11
MCF7	Valinomycin 100 nM	91

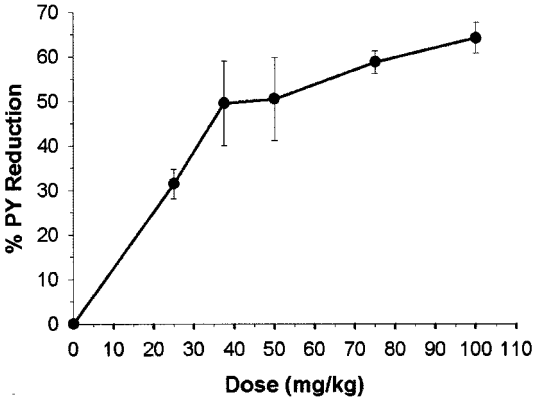

Fig. 9. CP-654577 Produces a Dose-dependent Reduction of erbB2 Tyrosine Phosphorylation (PY) in FRE-erbB2 Tumors. Briefly, 5×10^5 FRE erbB2 cells were injected s.c. into athymic mice. When the tumors reached ~300 mm^3 (15–18 days) in volume, CP-654577 was administered i.p. in 5% Gelucire (44/14; Gattefosse Inc.)/95% sterile water at doses of 25, 37.5, 50, 75, and 100 mg/kg. Tumors were collected 2 h postdose. The tumor lysates were analyzed for reduction of erbB2 phosphorylation as described in "Materials and Methods." The values are the average ± SE, $n = 4$.

Downloaded from http://aacrjournals.org/cancerres/article-pdf/63/15/4450/2505431/ch1503004450.pdf by guest on 22 June 2024

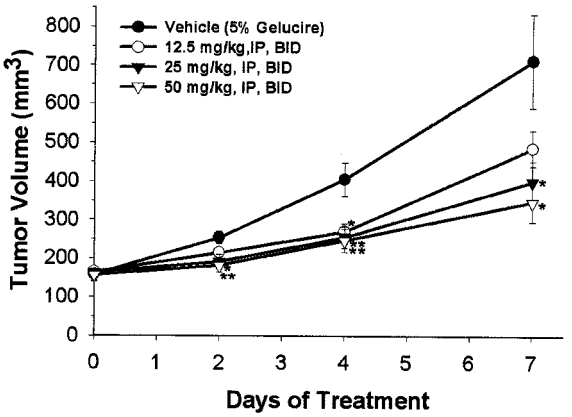

Fig. 10. CP-654577 Produces a Dose-dependent Inhibition of erbB2-driven Tumor Growth. Mice bearing FRE-erbB2 tumors of ~150 mm^3 in size (10 days after inoculation as described in "Materials and Methods") were treated with vehicle or CP-654577 in 5% Gelucire at 12.5, 25, and 50 mg/kg twice daily by i.p. injection for 7 days. Tumor volume (mm^3) was calculated as described under "Materials and Methods" on days 2, 4, and 7. Each group contained nine or ten mice. Values are provided as mean ± SE. Significance compared with vehicle-treated controls (*, $P < 0.05$; **, $P < 0.01$) was determined by Students *t* test. No mortality of the animals was noted in any groups. Furthermore, no weight loss was observed in any group; the average mouse weight in the highest dose group (50 mg/kg) was 21.50 g at the outset of the experiment and was 21.53 at the conclusion of the study.

levels of phosphorylated erbB2 receptor in tumors in a dose-dependent manner within 2 h of administration (Fig. 9). The dose that caused 50% reduction in the level of erbB2 phosphorylation relative to vehicle-treated controls was calculated to be 43 mg/kg.

The FRE/erbB2 tumor model was also used to evaluate the antitumor efficacy of CP-654577 (Fig. 10). CP-654577 produced a dose-dependent inhibition of FRE/erbB2 tumor growth with efficacy observed within two days of dosing at the two higher doses. On Day 7, we observed 40%, 58%, and 65% inhibition of growth (relative to vehicle-treated controls) at 12.5, 25, and 50 mg/kg, IP, BID, respectively. Thus CP-654577 is a potent inhibitor of erbB2 phosphorylation in tumor xenografts and this inhibition translates into antitumor efficacy against erbB2-driven tumor growth.

DISCUSSION

Many tyrosine kinases are important in the regulation of cell proliferation, and thus have been targeted for antiproliferative drug discovery. This approach has met with considerable success; both therapeutic antibodies and low molecular weight kinase inhibitors have been approved for use. Most of the tyrosine kinase inhibitors reported to date have been competitive inhibitors with respect to ATP and are presumed to bind at the ATP site of the kinases. Despite the high conservation of sequence in the kinase domains of tyrosine kinases, considerable selectivity of inhibitors has been obtained. For example, Tarceva is >1000-fold more potent *versus* EGFr than against *c-src* or *v-abl* tyrosine kinases (12) and PKI166 is >1000-fold selective for EGFr relative to flk, c-met, or Tek kinases (35). The problem of identifying selective inhibitors for very closely related proteins such as EGFr and erbB2 would be expected to be more difficult because of the very high (82%) amino acid sequence identity in the kinase domains (3).

Contrary to that expectation, the EGFr inhibitor Tarceva is >100-fold selective for EGFr kinase *versus* erbB2 kinase in assays comparing activity of their intracellular domains (Fig. 1; see Ref. 36) and considerable selectivity is also seen in cellular assays (Figs. 2 and 3; Table 1). Through an extensive medicinal chemistry effort we have identified structural modifications that reduce EGFr kinase inhibition while enhancing erbB2 inhibition.[3] This process has identified new inhibitors that have an opposite selectivity relative to Tarceva, *i.e.*, erbB2 selective inhibitors, exemplified here by CP-654577. This compound is ~60-fold selective for erbB2 relative to EGFr in assays of isolated kinase (Fig. 1) and this selectivity is also apparent in cell-based assays (Figs. 2 and 3; Table 1).

The distinct selectivity of Tarceva and CP-654577 result in markedly different patterns of biochemical effects upon treatment of cells that express both EGFr and erbB2 such as SKBr3 cells. Analysis of tyrosine phosphorylation of the erbB proteins in these cells show that CP-654577 is markedly more potent than Tarceva in reducing erbB2 and erbB3 phosphorylation (Fig. 3*B*). SKBr3 cells express high levels of erbB2 and the basal erbB2 tyrosine phosphorylation presumably results from erbB2 transphosphorylation within homodimers, whereas the phosphorylation of the kinase inactive erbB3 results from transphosphorylation by erbB2 in erbB2/erbB3 heterodimers. Conversely, Tarceva is markedly more potent in the suppression of EGF-induced EGFr tyrosine phosphorylation (Fig. 3*D*). This phosphorylation results from EGFr transphosphorylation in EGFr homodimers. The distinct selectivity of Tarceva and CP-654577 is also clear from the analysis of "downstream" signaling events. CP-654577 reduces MAPK activation (Fig. 6*C*) and Akt activation (Fig. 7*C*) at lower concentrations than Tarceva. Conversely, Tarceva is a more potent inhibitor of EGF-induced activation of MAPK (Fig. 6*C*) and Akt (Fig. 7*C*).

A recent study of selectivity of anilino-quinazoline inhibitors also found that low molecular weight substitutions on the aniline resulted in inhibitors with selectivity for EGFr relative to erbB2 kinase, and that this differential was reduced by aromatic substitutions in the anilino moiety. The resulting inhibitors were approximately equipotent for EGFr and erbB2 (37). In addition, this group has identified pyrido-pyrimidine-based inhibitors, ex. GW2974, that are also equipotent erbB2/EGFr inhibitors (36).

The selectivity of CP-654577 for erbB2 relative to EGFr distinguishes it not only from Tarceva and GW2974, but also from other published reversible EGFr inhibitors such as Iressa (~100-fold EGFr-selective, Ref. 17) or PKI166 (~ 11-fold EGFr-selective, Ref. 35). Irreversible inhibitors active against both EGFr and erbB2 have also been reported, and appear to have only limited selectivity between the two kinases (18, 19). A study of two EGFr kinase inhibitors, PD153035 and BIBX1382BS, in whole cell assays found little selectivity for the former and a modest (~3-fold) selectivity of the latter for EGFr (38). CP-654577 therefore is a novel inhibitor with considerable selectivity for erbB2 relative to EGFr.

A model for the biological and biochemical effects of CP-654577 demonstrated by these studies is provided as Fig. 11. Treatment of SKBr3 cells leads to decreased phosphorylation of erbB2 and erbB3, resulting in decreased levels of activated MAPK and Akt. This in turn results in decreased cyclin D and increased $p27^{kip1}$, impeding phosphorylation of RB and entry into S phase. Apoptosis also contributes to the overall reduction in rate of tumor cell increase.

CP-654577 inhibits SKBr3 proliferation by blocking cell cycle progression in the G_1 phase (Fig. 5). Reduction of erbB2 activity by antisense (33), antibodies targeting erbB2 to the endoplasmic reticulum (23), AG1478 an EGFr-selective kinase inhibitor with lower potency against erbB2 kinase (39) or anti-$p185^{erbB2}$ antibodies, including the clinical agent trastuzumab, also produce a G_1 block (40–42). Cell-cycle progression past the G_1 "restriction point" requires phosphorylation of Rb protein, initiated by cyclin D/cdk2 and

[3] S. K. Bhattacharya, E. D. Cox, J. C. Kath, A. M. Mathiowetz, J. Morris, J. D. Moyer, L. R. Pustilnik, K. Rafidi, D. T. Richter, C. Su, and M. D. Wessel, manuscript in preparation.

Downloaded from http://aacrjournals.org/cancerres/article-pdf/63/15/4450/2505431/ch1503004450.pdf by guest on 22 June 2024

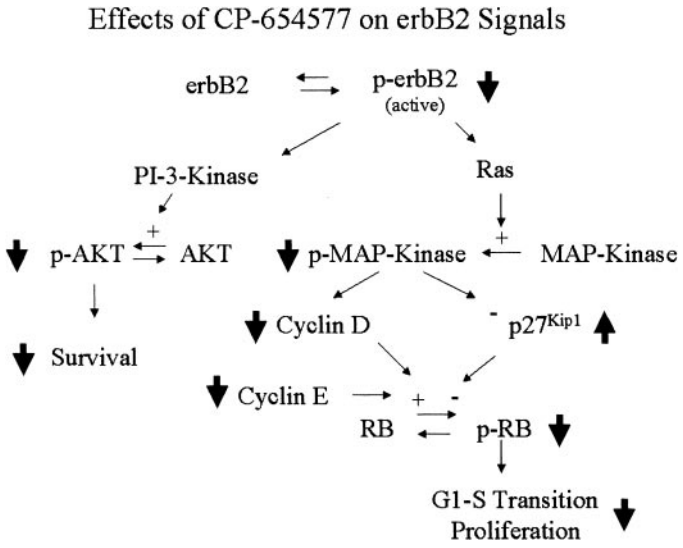

Fig. 11. Effects of CP-654577 on erbB2 signals. Selected biochemical signaling pathways linked to erbB2 (1, 2) are shown. The changes documented in this report to occur in SKBr3 cells in response to CP-654577 are indicated by the bold arrows: decreases in phosphorylated erbB2, activated MAP-kinase, cyclinD, cyclinE, pRB, S-phase cells, activated AKT, and survival, together with an increase in $p27^{kip1}$.

then accelerated by cyclin E/cdk2 as cyclin E levels climb in late G_1 (29). The cyclinD/cdk2 activity is further regulated by the inhibitory effect of $p27^{kip1}$. Inhibition of erbB2 kinase by CP-654577 leads to a reduction in levels of the permissive (hyper-phosphorylated) form of Rb (Fig. 5*A*) possibly as a consequence of loss of cyclin D (Fig. 5*D*) and cyclin E (Fig. 5*C*), and an increase in $p27^{kip1}$ (Fig. 5*B*). Reduction of erbB2 activity by the other approaches noted above also reduced RB phosphorylation (23, 41), cyclin D (23, 42, 43), and cyclin E kinase activity (23), and increased $p27^{kip1}$ (40, 41, 43). An understanding of the relative contributions of these biochemical effects of erbB2 inhibition to the cell cycle block produced by CP-654577 requires further study.

Signals from erbB2 can activate the MAPK pathway and the PI-3-kinase pathway (1). SKBr3 cells have both activated MAPK and Akt (Figs. 6 and 7) that are greatly reduced by CP-654577 exposure. The levels of cyclin D can be positively regulated by both transcriptional effects of MAPK activation (1) and by stabilization of cyclin D protein by activity of the Akt pathway (44). Thus the decreased levels of cyclin D upon treatment with CP-654577 may be mediated by the resulting decreased activity of MAPK and Akt. Recent studies by Yakes *et al.* (43) implicate the effect on Akt as crucial in trastuzumab induced cell cycle blockade and cyclin D depletion. Enforced high expression of cyclin D reverses the antiproliferative effects of the EGFr/erbB2 inhibitor AG1478 in BT474 cells (39); this suggests that depletion of cyclin D may be the crucial mediator of the antiproliferative effect of erbB2 inhibition.

In addition to the role of erbB2 in cell proliferation, signals originating from erbB2 promote cell survival (31–33) and the erbB2/erbB3 heterodimer has been shown to have particularly strong anti-apoptotic activity (45). Inhibition of erbB2 by CP-654577 induced apoptosis in SKBr3 and BT474 cells at sub-micromolar concentrations, but did not induce apoptosis in MCF7 cells, a line that expresses much lower levels of erbB2 (Fig. 8; Table 2). The degree of induction of apoptosis in SKBr3 cells by CP-654577 was ~3-fold at 1 μM, somewhat higher or similar to the induction reported for trastuzumab (34, 43). The induction of apoptosis by trastuzumab in SKBr3 cells was shown to be reversed by transfection of an activated form of Akt, thus identifying the indirect inhibition of Akt as the key mechanism of induction of apoptosis in these cells (43). Inhibition of erbB2 by antisense or anti-erbB2 antibodies enhances induction of apoptosis by doxorubicin (23) and TRAIL (34); thus, combinations of an erbB2 inhibitor such as CP-654577 and other chemotherapeutic agents may enhance tumor cell death.

The selectivity of CP-654577 for erbB2 *versus* EGFr distinguishes it from other reported inhibitors selective for EGFr or similarly active against both EGFr and erbB2. A selective erbB2 inhibitor with reduced activity against EGFr such as CP-654577 may avoid some of the toxicity observed with EGFr inhibitors, notably the acneiform skin rash produced by the EGFr inhibitors Tarceva, gefitinib, and C225 (5, 15), but not observed with the anti-erbB2 antibody trastuzumab (7, 8). Although the current experiments demonstrate that CP-654577 has antitumor activity in an erbB2-driven tumor (Fig. 10), we have not yet evaluated it against a panel of tumors with diverse expression of EGFr and erbB2 to demonstrate that this biochemical selectivity translates to a distinct pattern of therapeutic efficacy relative to EGFr selective inhibitors. This question is further complicated by the coexpression of the various erbB proteins at diverse ratios in human clinical tumors. However, the observed biochemical selectivity, together with its potent antiproliferative effects on erbB2-dependent cells *in vitro* (SKBr3 cells) and *in vivo* (FRE-ErbB2 tumors), makes this class of erbB2-selective inhibitors attractive for further development as potential antitumor agents.

REFERENCES

1. Yarden, Y., and Sliwkowski, M. X. Untangling the *erb*B signalling network. Mol. Cell. Biol., *2:* 127–137, 2001.
2. Hynes, N. E., and Stern, D. F. The biology of *erb*B-2/*neu*/HER-2 and its role in cancer. Biochim. Biophys. Acta, *1198:* 165–184, 1994.
3. Prigent, S. A., and Lemoine, N. R. The Type-1 (EGFR-related) family of growth factor receptors and their ligands. Prog. Growth Factor Res., *4:* 1–24, 1992.
4. Baselga, J., and Mendelsohn, J. Type I receptor tyrosine kinases as targets for therapy in breast cancer. J. Mammary Gland Biol. Neoplasia, *2:* 165–174, 1997.
5. Slichenmyer, W., and Fry, D. W. Anticancer therapy targeting the ErbB family of receptor tyrosine kinases. Semin. Oncol., *28* (Suppl. 16)*:* 67–79, 2001.
6. Mendelsohn, J. The epidermal growth factor receptor as a target for cancer therapy. Endocr. Relat. Cancer, *8:* 3–9, 2001.
7. Baselga, J., Tripathy, D., Mendelsohn, J., Baughman, S., Benz, C. C., Dantis, L., Sklarin, N. T., Seidman, A. D., Hudis, C. A., Moore, J., Rosen, P. P., Twaddell, T., Henderson, I. C., and Norton, L. Phase II study of weekly intravenous trastuzumab (Herceptin) in patients with HER2/*neu*-overexpressing metastatic breast cancer. Semin. Oncol., *26:* 78–83, 1999.
8. Slamon, D. J., Leyland-Jones, B., Shak, S., Fuchs, H., Paton, V., Bajamonde, A., Fleming, T., Eierman, W., Wolter, J., Pegram, M., Baselga, J., and Norton, L. Use of chemotherapy plus a monoclonal antibody against HER2 for metastatic breast cancer that overexpresses HER2. N. Eng. J. Med., *344:* 783–792, 2001.
9. Vogel, C. L., Cobleigh, M. A., Tripathy, D., Gutheil, J. C., Harris, L. N., Fehrenbacher, L., Slamon, D. J., Murphy, M., Novotny, W. F., Burchmore, M., Shak, S., and Stewart, S. J. First-Line Herceptin® monotherapy in metastatic breast cancer. Oncology, *61* (Suppl. 2)*:* 37–42, 2001.
10. Baselga, J., Pfister, D., Cooper, M. R., Cohen, R., Burtness, B., Bos, M., D'Andrea, G., Seidman, A., Norton, L., Gunnett, K., Falcey, J., Anderson, V., Waksal, H., and Mendelsohn, J. Phase I studies of anti-epidermal growth factor receptor chimeric antibody C225 alone and in combination with cisplatin. J. Clin. Oncol., *18:* 904–914, 2000.
11. Ciardiello, F., and Tortora, G. A novel approach in the treatment of cancer: targeting the epidermal growth factor receptor. Clin. Cancer Res., *7:* 2958–2970, 2001.
12. Moyer, J. D., Barbacci, E. G., Iwata, K. K., Arnold, L., Boman, B., Cunningham, A., DiOrio, C., Doty, J., Morin, M. J., Moyer, M. P., Neveu, M., Pollack, V. A., Pustilnik, L. R., Reynolds, M. M., Sloan, D., Theleman, A., and Miller, P. Induction of apoptosis and cell cycle arrest by CP-358,774, an inhibitor of epidermal growth factor receptor tyrosine kinase. Cancer Res., *57:* 4838–4848, 1997.
13. Pollack, V. A., Savage, D. M., Baker, D. A., Tsaparikos, K. E., Sloan, D. E., Moyer, J. D., Barbacci, E. G., Pustilnik, L. R., Smolarek, T. A., Davis, J. A., Vaidya, M. P., Arnold, L. D., Doty, J. L., Iwata, K. K., and Morin, M. J. Inhibition of epidermal growth factor receptor-associated tyrosine phosphorylation in human carcinomas with CP-358,774: dynamics of receptor inhibition in situ and antitumor effects in athymic mice. J. Pharmacol. Exper. Ther., *291:* 739–748, 1999.
14. Perez-Soler, R., Chachoua, A., Huberman, M., Karp, D., Rigas, J., Hammond, L., Rowinsky, E., Preston, G., Ferrante, K., Allen, L. F., Nadler, P. I., and Bonomi, P. A Phase II trial of the epidermal growth factor receptor (EGFR) tyrosine kinase inhibitor OSI-774, following platinum-based chemotherapy, in patients with advanced EGFR-expressing nonsmall cell cancer. Proc. Am. Soc. Clin. Oncol., *20:* 310a, 2001.
15. Ciardello, F., Caputo, R., Bianco, R., Damiano, V., Pomatico, G., DePlacido, S., Bianco, A. R., and Tortora, G. Antitumor effect and potentiation of cytotoxic drugs

Downloaded from http://aacrjournals.org/cancerres/article-pdf/63/15/4450/2505431/ch1503004450.pdf by guest on 22 June 2024

activity in human cancer cells by ZD-1839 (Iressa), an epidermal growth factor receptor-selective tyrosine kinase inhibitor. Clin. Cancer Res., *6:* 2053–2063, 2000.
16. Moulder, S. L., Yakes, F. M., Muthuswamy, S. K., Bianco, R., Simpson, J. F., and Arteaga, C. L. Epidermal growth factor receptor (HER1) tyrosine kinase inhibitor ZD1839 (Iressa) inhibits HER2/*neu* (*erb*B2)-overexpressing breast cancer cells *in vitro* and *in vivo*. Cancer Res., *61:* 8887–8895, 2001.
17. Woodburn, J., Kendrew, J., Fennell, M., Kelly, H., and Wakeling, A. ZD1839 ('Iressa'), a selective epidermal growth factor receptor tyrosine kinase inhibitor (EGFR-TKI): correlation of c-*fos* expression and tumor growth inhibition. Proc. Am. Assoc. Cancer Res., *41:* 406, 2000.
18. Tsou, H-W, Mamuya, N., Johnson, B. D., Reich, M. F., Gruber, B. C., Ye, F., Nilakantan, R., Shen, R., Discafani, C., DeBlanc, R., Davis, R., Koehn, F. E., Greenberger, L. M., Wang, Y-F., and Wissner, A. 6-Substituted-4-(3-bromophenylamino)quinazolines as putative irreversible inhibitors of the epidermal growth factor receptor (EGFR) and human epidermal growth factor receptor (HER-2) tyrosine kinases with enhanced antitumor activity. J. Med. Chem., *44:* 2719–2734, 2001.
19. Fry, D. W., Bridges, A. J., Denny, W. A., Doherty, A., Greis, K. D., Hicks, J. L., Hook, K. E., Keller, P. R., Leopold, W. R., Loo, J. A., McNamara, D. J., Nelson, J. M., Sherwood, V., Smaill, J. B., Trumpp-Kallmeyer, S., and Dobrusin, E. M. Specific, irreversible inactivation of the epidermal growth factor receptor and *erb*B2, by a new class of tyrosine kinase inhibitor. Proc. Nat. Acad. Sci., USA, *95:* 12022–12027, 1999.
20. Colomer, R., Lupu, R., Bacus, S. S., and Gelmann, E. P. *erb*B-2 antisense oligonucleotides inhibit the proliferation of breast carcinoma cells with *erb*B-2 oncogene amplification. Br. J. Cancer, *70:* 819–825, 1994.
21. Lewis, G. D., Figari, I., Fendly, B., Wong, W. L., Carter, P., Gorman, C., and Shepard, H. M. Differential responses of human tumor cell lines to anti-p185HER2 monoclonal antibodies. Cancer Immunol. Immunother., *37:* 255–263, 1993.
22. Hudziak, R. M., Lewis, G. D., Winget, M., Fendly, B. M., Shepard, H. M., and Ullrich, A. p185HER2 monoclonal antibody has antiproliferative effects *in vitro* and sensitizes human breast tumor cells to tumor necrosis factor. Mol. Cell. Biol., *9:* 1165–1172, 1989.
23. Neve, R. M., Sutterluty, H., Pullen, N., Lane, H. A., Daly, J. M., Krek, W., and Hynes, N. E. Effects of oncogenic ErbB2 on G_1 cell cycle regulators in breast tumour cells. Oncogene, *19:* 1647–1656, 2000.
24. Kath, J. C., Tom, N. J., Cox, E. D., and Bhattacharya, S. K. Preparation of aminoquinazolines and related compounds as anticancer drugs. Eur. Pat. Appl., EP 1029853, 2000.
25. Faziloi, F., Kim, U-H., Rhee, S. G., Molloy, C. J., Segatto, O., and DiFiore, P. P. The *erb*B-2 mitogenic signalling pathway: tyrosine phosphorylation of phospholipase C-g and GTPase-activating protein does not correlate with *erb*B-2 mitogenic potency. Mol. Cell. Biol., *11:* 2040–2048, 1991.
26. Cohen, B. D., Goldstein, D. J., Rutledge, L., Vass, W. C., Lowy, D. R., Schlegel, R., and Schiller, J. T. Transformation specific interaction of the bovine papilomavirus E5 oncoprotein with the platelet-derived growth factor receptor transmembrane domain and the epidermal growth factor receptor cytoplasmic domain. J. Virol., *67:* 5303–5311, 1993.
27. Association for Assessment and Accreditation of Laboratory Animal Care. Guide for the Care and Use of Laboratory Animals, Ed. 6. National Academy Press, Washington D. C., 1996.
28. Brockhoff, G., Heisz, P., Schlegel, J., Hofstaedter, F., and Knuecchel, R. Epidermal growth factor receptor, c-*erb*B2 and c-*erb*B3 receptor interaction, and related cell cycle kinetics of SK-BR-3 and BT474 breast carcinoma cells. Cytometry, *44:* 338–348, 2001.
29. Weinberg, R. A. The retinoblastoma protein and cell cycle control. Cell, *81:* 323–330, 1995.
30. Wilkinson, M. G., and Millar, J. B. Control of the eukaryotic cell cycle by MAP kinase signaling pathways. FASEB J., *14:* 2147–2157, 2000.
31. Roh, H., Pippin, J., and Drebin, J. A. Down-regulation of HER2/*neu* expression induces apoptosis in human cancer cells that overexpress HER2/*neu*. Cancer Res., *60:* 560–565, 2000.
32. Zhou, B. P., Hu, M. C-T., Miller, S. A., Yu, Z., Xia, W., Lin, S.-Y, and Hung, M-C. HER-2/*neu* blocks tumor necrosis factor-induced apoptosis via the Akt/NF-κB pathway. J. Biol. Chem., *275:* 8027–8031, 2000.
33. Roh, H., Pippin, J. A., Green, D. W., Boswell, C. B., Hirose, C. T., Mokadam, N., and Drebin, J. A. HER2/*neu* antisense targeting of human breast carcinoma. Oncogene, *19:* 6138–6143, 2000.
34. Cuello, M., Ettenberg, S. A., Clark, A. S., Keane, M. C., Posner, R. H., Nau, M. N., Dennis, P. A., and Lipkowitz, S. Down-regulation of the *erb*B2 receptor by trastuzumab (Herceptin) enhances tumor necrosis factor-related apoptosis-inducing ligand-mediated apoptosis in breast and ovarian cancer cell lines that overexpress *erb*B2. Cancer Res., *61:* 4892–4900, 2001.
35. Traxler, P., Bold, G., Buchdunger, E., Caravatti, G., Furet, P., Manley, P., O'Reilly, T., Wood, J., and Zimmermann, J. Tyrosine kinase inhibitors: from rational design to clinical trials. Med. Res. Rev., *21:* 499–512, 2001.
36. Rusnak, D. W., Affleck, K., Cockerill, S. G., Stubberfield, C., Harris, R., Page, M., Smith, K. J., Guntrip, S. B., Carter, M. C., Shaw, R. J., Jowett, A., Stables, J., Topley, P., Wood, E. R., Brignola, P. S., Kadwell, S. H., Reep, B. R., Mullin, R. J., Alligood, K. J., Keith, B. R., Crosby, R. M., Murray, D. M., Knight, W. B., Gilmer, T. M., and Lackey, K. The characterization of novel, dual ErbB-2/EGFR, tyrosine kinase inhibitors: potential therapy for cancer. Cancer Res., *61:* 7196–7203, 2001.
37. Brignola, P. S., Lackey, K., Kadwell, S. H., Hoffman, C., Horne, E., Carter, H. L., Stuart, J. D., Blackburn, K., Moyer, M. P., Alligood, K. J., Knight, W. B., and Wood, E. R. Comparison of the biochemical and kinetic properties of the type 1 receptor tyrosine kinase intracellular domains. J. Biol. Chem., *277:* 1576–1585, 2002.
38. Egeblad, M., Mortensen, O. H., van Kempen, L. C., and Jaattela, M. BIBX1382BS, but not AG1478 or PD153035, inhibits the ErbB kinases at different concentrations. Biochem. Biophys. Res. Commun., *281:* 25–31, 2001.
39. Lenferink, A. E. G., Busse, D., Flanagan, W. M., Yakes, F. M., and Arteaga, C. L. ErbB2/*neu* kinase modulates cellular p27Kip1 and cyclin D1 through multiple signaling pathways. Cancer Res., *61:* 6583–6591, 2001.
40. Sliwkowski, M. X., Lofgren, J. A., Lewis, G. D., Hotaling, T. E., Fendly, B. M., and Fox, J. A. Nonclinical studies addressing the mechanism of action of trastuzumab (Herceptin). Semin. Oncol., *26:* 60–70, 1999.
41. Le, X. F., McWatters, A., Wiener, J., Wu, J. Y., Mills, G. B., and Bast, R. C., Jr. Anti-HER2 antibody and heregulin suppress growth of HER2-overexpressing human breast cancer cells through different mechanisms. Clin. Cancer Res., *6:* 260–270, 2000.
42. Lane, H. A., Beuvink, I., Motoyama, A. B., Daly, J. M., Neve, R. M., and Hynes, N. E. ErbB2 potentiates breast tumor proliferation through modulation of p27(Kip1)-Cdk2 complex formation: receptor over-expression does not determine growth dependency. Mol. Cell. Biol., *20:* 3210–3223, 2000.
43. Yakes, F. M., Chinratanalab, W., Ritter, C. A., King, W., Seelig, S., and Arteaga, C. L. Herceptin-induced inhibition of phosphatidylinositol-3-kinase and Akt is required for antibody-mediated effects on p27, cyclin D1 and antitumor action. Cancer Res., *62:* 4132–4141, 2002.
44. Diehl, J. A., Cheng, M., Roussel, M. F., and Sherr, C. J. Glycogen synthase kinase-3β regulates cyclin D1 proteolysis and subcellular localization. Genes Dev., *12:* 3499–3511, 1998.
45. Pinkus-Kramarski, R., Soussa, L., Waterman, H., Levkowitz, G., Alroy, I., Klapper, L., Lavi, S., Seger, R., Ratzkin, B. J., Sela, M., and Yarden, Y. Diversification of Neu differentiation factor and epidermal growth factor signaling by combinatorial receptor interactions. EMBO J., *15:* 2452–2467, 1996.

Downloaded from http://aacrjournals.org/cancerres/article-pdf/63/15/4450/2505431/ch1503004450.pdf by guest on 22 June 2024